Brain Structure and Function
https://doi.org/10.1007/s00429-022-02581-z

ORIGINAL ARTICLE

Distribution of vasopressin 1a and oxytocin receptor protein and mRNA in the basal forebrain and midbrain of the spiny mouse (*Acomys cahirinus*)

Jeanne M. Powell[1] · Kiyoshi Inoue[2,3] · Kelly J. Wallace[1] · Ashley W. Seifert[4] · Larry J. Young[2,3,5] · Aubrey M. Kelly[1]

Received: 22 August 2022 / Accepted: 7 October 2022

Abstract

The nonapeptide system modulates numerous social behaviors through oxytocin and vasopressin activation of the oxytocin receptor (OXTR) and vasopressin receptor (AVPR1A) in the brain. OXTRs and AVPR1As are widely distributed throughout the brain and binding densities exhibit substantial variation within and across species. Although OXTR and AVPR1A binding distributions have been mapped for several rodents, this system has yet to be characterized in the spiny mouse (*Acomys cahirinus*). Here we conducted receptor autoradiography and in situ hybridization to map distributions of OXTR and AVPR1A binding and *Oxtr* and *Avpr1a* mRNA expression throughout the basal forebrain and midbrain of male and female spiny mice. We found that nonapeptide receptor mRNA is diffuse throughout the forebrain and midbrain and does not always align with OXTR and AVPR1A binding. Analyses of sex differences in brain regions involved in social behavior and reward revealed that males exhibit higher OXTR binding densities in the lateral septum, bed nucleus of the stria terminalis, and anterior hypothalamus. However, no association with gonadal sex was observed for AVPR1A binding. Hierarchical clustering analysis further revealed that co-expression patterns of OXTR and AVPR1A binding across brain regions involved in social behavior and reward differ between males and females. These findings provide mapping distributions and sex differences in nonapeptide receptors in spiny mice. Spiny mice are an excellent organism for studying grouping behaviors such as cooperation and prosociality, and the nonapeptide receptor mapping here can inform the study of nonapeptide-mediated behavior in a highly social, large group-living rodent.

Keywords Vasopressin · Oxytocin · Receptor autoradiography · In situ hybridization · Social behavior · Spiny mouses

Abbreviations

AOB	Accessory olfactory bulb
aco	Anterior commissure
AI	Agranular insular area of the cortex
AHAL	Amygdalohippocampal area, anterolateral part
AH	Anterior hypothalamus
AOA	Anterior olfactory areas
APT	Anterior pretectal nucleus
BLA	Basolateral amygdala
BNST	Bed nucleus of the stria terminalis
BNSTa	Bed nucleus of the stria terminalis, anterior division
BNSTp	Bed nucleus of the stria terminalis, posterior division
CPu	Caudate putamen
CeA	Central amygdala
Cg	Cingulate cortex
cc	Corpus callosum
Cg2	Cortical layer 2
Cg5	Cortical layer 5
DG	Dentate gyrus
VDB	Diagonal band nucleus
DI	Dysgranular insular cortex
GP	Globus pallidus

✉ Aubrey M. Kelly
aubrey.kelly@emory.edu

[1] Department of Psychology, Emory University, 36 Eagle Row, Atlanta, GA 30322, USA

[2] Center for Translational Social Neuroscience, Emory University, Atlanta, GA 30329, USA

[3] Emory National Primate Research Center, Emory University, Atlanta, GA 30329, USA

[4] Department of Biology, University of Kentucky, 101 Morgan Building, Lexington, KY 40506, USA

[5] Department of Psychiatry and Behavioral Sciences, Emory University School of Medicine, Atlanta, GA 30322, USA

Published online: 21 October 2022

Hi	Hippocampus
CA1	Hippocampal field CA1
CA1py	Hippocampal field CA1 pyramidal layer
CA3	Hippocampal field CA3
IP	Interpeduncular nucleus
LD	Lateral dorsal nucleus of thalamus
LH	Lateral hypothalamus
LS	Lateral septum
LSc	Lateral septum, caudo-dorsal region
LSv	Lateral septum, ventral region
MOB	Main olfactory bulb
MOBgl	Main olfactory bulb, glomerular layer
MOBgr	Main olfactory bulb, granule layer
MeA	Medial amygdala
MG	Medial geniculate nucleus of the thalamus
MM	Medial mammillary nucleus of the hypothalamus
MPOA	Medial preoptic area of the hypothalamus
NAcc	Nucleus accumbens
OT	Olfactory tubercle
och	Optic chiasm
PV	Paraventricular thalamic nucleus
PVA	Paraventricular thalamic nucleus, anterior division
PAG	Periaqueductal gray
PVG	Periventricular gray
PIR	Piriform area
Re	Reuniens thalamic nucleus
SC	Superior colliculus
SuG	Superior colliculus, superficial gray, sensory related
SCm	Superior colliculus, motor related
SCN	Suprachiasmatic nucleus of the hypothalamus
TT	Taenia tecta
3 V	Third ventricle
VPL	Ventral posterolateral nucleus of the thalamus
VMH	Ventromedial hypothalamic nucleus
VPall	Ventral pallidum
VIS	Visual areas of the cortex
ZI	Zona incerta

Introduction

The nonapeptides oxytocin (OXT) and vasopressin (AVP) modulate numerous social behaviors ranging from affiliation and pair bonding to anxiety and aggression (Albers 2012; Donaldson and Young 2008; Veenema and Neumann 2008; Rigney et al. 2022). OXT and AVP are produced in distinct populations in the hypothalamus, primarily those of the paraventricular and supraoptic nuclei, as well as in extrahypothalamic regions, and act on the OT-receptor (OXTR) and AVP1a-receptor (AVPR1A) via direct projections and dendritic release (Kelly and Goodson 2014; Ludwig and Leng 2006; Rood and De Vries 2011). Although the nonapeptide system is strongly conserved across vertebrates, there is substantial variation in receptor distributions and densities. Comparative and experimental studies have revealed that differences in OXTR and AVPR1A neuroanatomical distributions reflect differences in social phenotype observed both across and within species (Caldwell 2017; Goodson et al. 2009; Young and Wang 2004; Campbell et al. 2009). For example, differences in nonapeptide receptor densities have been causally linked to differences in the expression of monogamy-related behaviors, such as pair bonding, within and across monogamous and non-monogamous *Microtus* vole species (Barrett et al. 2013; Lim et al. 2004; Walum and Young 2018). Additionally, while some species, such as the prairie voles (Froemke and Young 2021), exhibit dense OXTR binding in the nucleus accumbens (NAcc), a region critical for social reward (Liu and Wang 2003), laboratory mice and social tuco-tucos exhibit no detectable OXTR binding in this region (Beery et al. 2008; Borie et al. 2022b). Because of this variation across species, it is important to characterize nonapeptide receptor distributions in a species prior to examining nonapeptide-mediated behavior.

Nonapeptide receptor distributions have been characterized in a multitude of rodents including prairie voles, pine voles, montane voles, meadow voles, Taiwan voles, tuco-tucos, naked mole rats, ground squirrels, laboratory rats, singing mice, California mice, Syrian hamsters, and laboratory mice (Beery et al. 2008; Bester-Meredith et al. 1999; Campbell et al. 2009; Chappell et al. 2016; Freeman et al. 2019; Insel et al. 1994; Kalamatianos et al. 2010; Mitre et al. 2016; Smith et al. 2017; Taylor et al. 2020; Young 1999; Inoue et al. 2022). However, OXTR and AVPR1A distributions have yet to be characterized in the spiny mouse (*Acomys cahirinus*), an emerging rodent model in the field of social neuroscience (Fricker et al. 2021; Gonzalez Abreu et al. 2022; Kelly and Seifert 2021).

Spiny mice were historically used as a disease model to study diabetes progression (Gonet et al. 1966; Shafrir 2000), but have emerged as a model for studying complex tissue regeneration given their remarkable ability to regenerate skin and musculoskeletal (Gawriluk et al. 2016; Seifert et al. 2012). Beyond organ regeneration, these rodents also exhibit unique cytoprotective features that provide enhanced repair of major internal organs and the central nervous system (Koopmans et al. 2021; Nogueira-Rodrigues et al. 2022; Okamura et al. 2021; Peng et al. 2021; Saxena et al. 2019). Spiny mice have also become an excellent model for studying human-like reproductive biology, particularly their demonstration of a menstrual cycle (Bellofiore et al. 2017, 2018). Furthermore, spiny mice are also an exciting model for developmental studies given their precocial mode of development (Brunjes 1990; Haughton et al. 2016).

Spiny mice are cooperative breeders that live in large colonies nested within rocky outcroppings in Africa, the Middle East, and southern Asia (Deacon 2009; Frynta et al. 2011; Nowak 1999). They are socially bold, highly prosocial, and exhibit little aggression in both reproductive and nonreproductive contexts with both novel and familiar conspecifics (Fricker et al. 2021; Gonzalez Abreu et al. 2022). Spiny mouse males and females provide alloparental care to unrelated neonates at an equal rate to that of which they provide their own offspring (Porter et al. 1980; Tuckova et al. 2016), and established breeding groups will welcome a newcomer into the group; a behavior that is relatively rare among rodents (Cizkova et al. 2011). Spiny mice also exhibit a strong preference to affiliate with larger over smaller groups (referred to as gregariousness) (Fricker et al. 2021; Gonzalez Abreu et al. 2022), and thus are an excellent model for studying associative grouping and the relevant neural mechanisms that underlie these behaviors.

We previously mapped the distribution of nonapeptide-producing neuronal populations in spiny mice (Kelly and Seifert 2021); however, there remains a need to characterize distributions of nonapeptide receptors in this species. Thus, here we performed receptor-binding autoradiography and duplex in situ hybridization for OXTR and AVPR1A binding and *Oxtr* and *Avpr1a* mRNA to map the distribution of nonapeptide receptor binding and mRNA throughout the basal forebrain and midbrain of male and female spiny mice. Identifying sites of binding provides insight into where nonapeptides act upon functional receptors, whereas identifying sites of mRNA expression tells us where those receptors are synthesized.

In contrast, if binding is detected in regions where mRNA is not, it suggests the receptors detected in that area originate in another area and are transported down axons and act presynaptically (Inoue et al. 2022). Since nonapeptide receptor expression can be sexually dimorphic (Sharma et al. 2019; Young 1999), we also sought to examine associations with gonadal sex on OXTR and AVPR1A binding densities, focusing specifically on brain regions involved in social behavior and reward—collectively known as the Social Decision-Making Network (SDMN) (O'Connell and Hofmann 2011, 2012)—for which distributions of OXTR and AVPR1A receptors have been found throughout for many rodents (Albers 2015; Caldwell 2017; Smith et al. 2017).

Methods

Animals

All spiny mice in this study were derived from breeders obtained from the Seifert Lab at the University of Kentucky and maintained at Emory University. Sex was defined based on gonads, with males having testes present and females having ovaries present. Animals were housed in groups of 2–5 same-sex siblings in either a GR1800 Double Decker cages (Tecniplast, West Chester, PA, USA) or a standard polycarbonate rat cage. They were provided ad libitum water and Purina Prolab RMH 1000 (Lab Diet, St. Louis, MO, USA). The colony room was maintained at an ambient temperature of 24 °C ± 1 °C and kept on a 14 h:10 h light/dark cycle (lights on at 7:00 AM). All procedures were approved by the Institutional Animal Care and Use Committee of Emory University (Protocol 201,900,126).

Tissue preparation

All subjects were adults (female $n = 8$; male $n = 8$) aged between PND 60 and 250, with age spans equally representing the entire range for both males and females. Subjects were euthanized by CO_2 inhalation, and their brains were dissected and flash-frozen on powdered dry ice. The brains were then wrapped in tinfoil and stored in a −80 °C freezer. Brains were thawed to −20 °C and coronally cryosectioned at 20 µm thickness. Multiple series of each brain were collected at 200 µm intervals on to Superfrost Plus slides (Fisher Scientific Co., Pittsburgh, PA, USA). Brain-mounted slides were again stored in the −80 °C freezer until further processing.

Receptor autoradiography receptor-binding assays

Receptor binding autoradiography for OXTR and AVPR1A were performed as previously described (Ross et al. 2009) on two sets of tissue from each brain. Briefly, slides were thawed and then post-fixed in 0.1% paraformaldehyde for 2 min. They were washed in two changes of 50 mM Tris buffer for 10 min each and transferred to binding chambers where they were immersed in I-125 Tracer Buffer for 1 h. Slides labeled for OXTR and AVPR1A were exposed to 50 pM ^{125}I-ornithine vasotocin analog (I-125 OVTA, PerkinElmer, Waltham, MA, USA) and 50 pM ^{125}I-Linear V1a antagonist (I-125 LVA, Perkin Elmer, Waltham, MA, USA), respectively. Slides were then washed at 4 °C in four changes of Tris and Magnesium Chloride Buffer for 5 min each. They were then dipped in sterile ultra-pure deionized water and dried completely. Slides labeled for AVPR1A binding were exposed to BioMax MR film (Kodak, Rochester, NY, USA) for 4 days. Slides labeled for OXTR binding were exposed to film for 10 days.

Receptor autoradiography competitive binding assay

Competitive binding assays were performed using six series of adjacent tissue, three for the OXTR competitive binding

assay and three for the AVPR1A competitive binding assay. For both assays, 50 nM of unlabeled OXTR-selective agonist [Thr4, Gly7]OT (TGOT) (Bachem, Torrance, CA, USA) or Manning compound (Bachem, Torrance, CA, USA) was applied. Specific binding of I-125 OVTA was eliminated by the application of TGOT, but was not affected by the application of Manning Compound, confirming that I-125 OVTA is specific to the OXTR in the spiny mouse. Specific binding of I-125 LVA was only partially blocked by the application of Manning Compound and was not affected by the application of TGOT (Fig. 1).

Receptor autoradiography imaging and quantification

Films were placed on the Northern Light B95 Imaging Research Precision Illuminator (Imaging Research Inc., St. Catherines, Ontario, Canda) and imaged using a 55 mm

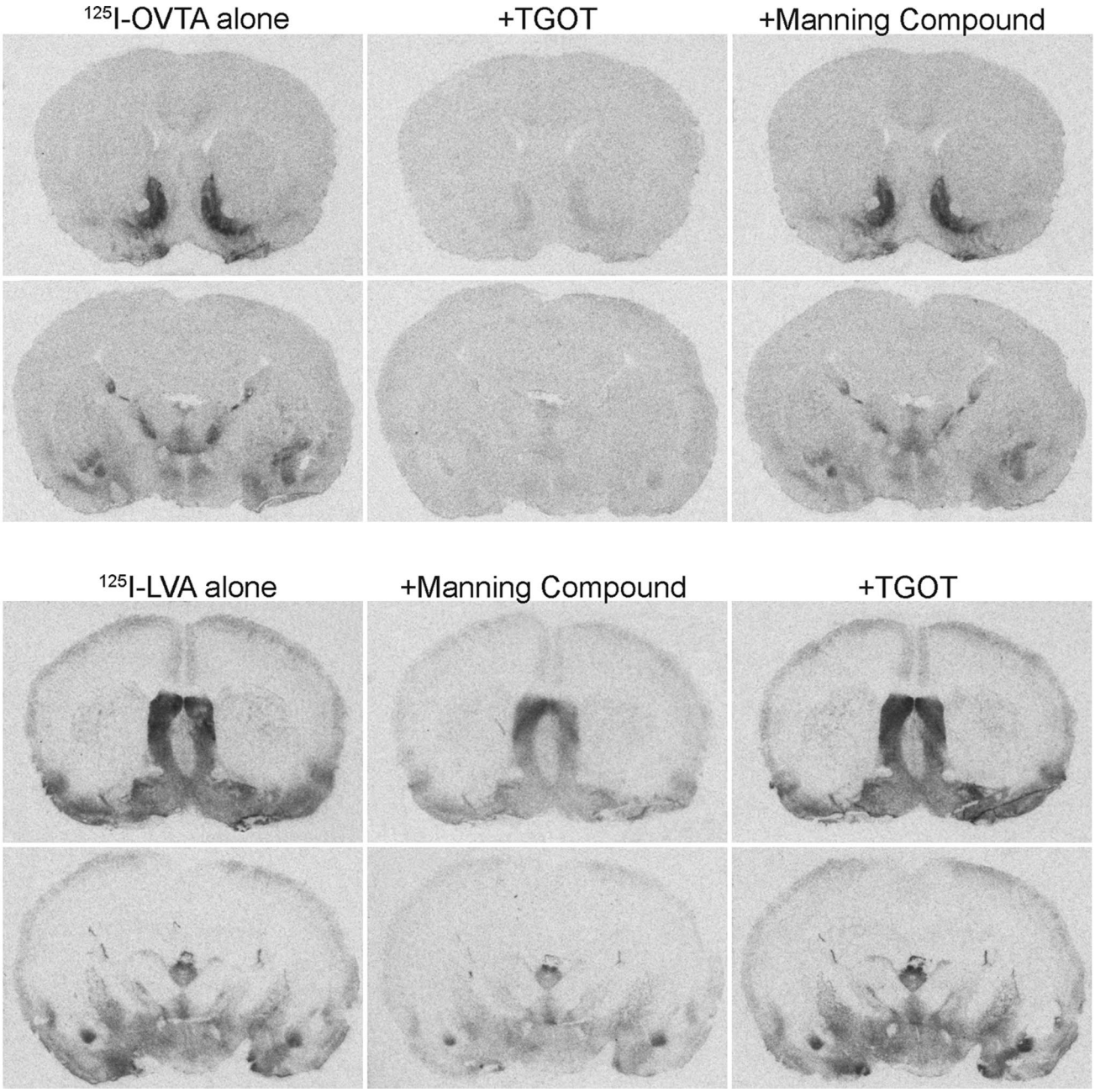

Fig. 1 *Autoradiograms of receptor binding in the presence or absence of receptor antagonists*. Application of TGOT, an oxytocin receptor antagonist, largely blocks I-OVTA binding in the spiny mouse. (Bottom) Application of Manning Compound, a V1a receptor antagonist, only partially blocks I-LVA binding in the spiny mouse

Nikon lens connected to QCapture Pro imaging software (Photometrics, Tucson, AZ, USA). All images were captured in the same sitting using the same illumination, focus, and exposure settings.

We sought to identify sex differences in brain regions involved in social behavior and reward and therefore focused on nodes within the SDMN, which included: nucleus accumbens (NAcc), lateral septum (LS), ventral pallidum (VPall), medial preoptic area (MPOA), bed nucleus of the stria terminalis (BNST), anterior hypothalamus (AH), basolateral amygdala (BLA), medial amygdala (MeA), caudate putamen (CPu), ventromedial hypothalamus (VMH), hippocampus (Hi), and periaqueductal gray (PAG). Regions of interest (ROIs) were identified by comparing dark regions on the autoradiographs to the Paxinos and Franklin Mouse Atlas, 5th edition (Paxinos and Franklin 2012) and images of the same or adjacent sections counterstained for Nissl. Receptor binding density was quantified in a semi-automated fashion using a custom FIJI macro (Schindelin et al. 2012). In this pipeline, images were automatically converted to an 8-bit grayscale format, with pixel grayscale values ranging from 0 to 255, where a value of 0 represents a black pixel (high radioactivity) and a value of 255 represents a white pixel (low radioactivity). ROIs were manually outlined using FIJI's freehand tool and then automatically renamed, measured, and saved based on user-provided information about the subject ID and ROI. Up to four measurements per subject were taken, two from the left and two from the right hemisphere, from intact sections capturing the ROI.

One ROI was used to determine background levels for the entire brain of each individual subject within an assay. To identify an appropriate background ROI, each image was pseudo-colored using the 16 color LUT. This allowed us to identify areas of intact gray matter that had the highest grayscale values (i.e., the least amount of radioactivity). Once identified, receptor binding density within the ROI was measured as described above. Visual cortex and the hippocampus were used as background ROIs for the OXTR and AVPR1A assays, respectively.

Each binding measurement was adjusted for background by taking the absolute value of the difference between the ROI's grayscale value and the subject-specific background value, resulting in a positive value. Then, an average for each ROI within each subject was taken. For the resulting data, a higher final grayscale value indicated higher receptor binding density.

In situ hybridization

Duplex in situ hybridization was performed on one set of tissue from the brains of three females and one male used in the autoradiography assays following a modified version of the RNAscope Multiplex Fluorescent Reagent Kit v2 Assay for Fresh-frozen Samples (technical bulletin #323,100-USM, Advanced Cell Diagnostics, Newark, CA, USA). Briefly, sections were fluorescently double-labeled for *Oxtr* and *Avpr1a* mRNA using RNAscope Probe—Ad-Oxtr (Part ID: 819,661-C2) and RNAscope Probe—Ad-Avpr1a (Part ID: 821,881), respectively. Probes were designed by ACD Inc. based off the following gene sequences from the spiny mouse genome:

Arginine vasopressin 1a receptor gene

ATGAGTTTCCCGCGAGGCTCCCACGATCGGCCC
GCGAGCAACTCCAGCCCGTGGTGGCCTCTGATC
GCCGCCGAGGGTGTCAACGCCAGCCGGGAGGCA
TCCGGGCTTGGGGAAGGTAGCGGCCCGCCAGGG
GATGTGCGCGATGAGGAGCTGGCCAAGGGGGAA
ATCGCTGTGCTGGCGGTGATTTTCGTGGTGGCTGTG
CTGGGCAATAGCAGTGTGCTGCTGGCGCTGCATCGC
ACGCCTCGCAAGACGTCCCGCATGCATCTCTTCATC
CGACACCTCAGCCTGGCAGACCTGGCGGTAGCCTTC
TTCCAAGTGCTGCCACAGCTGTGCTGGGACATCACC
TACCGCTTCCGCGGGCCGGACTGGCTGTGCCGCGTG
GTGAAGCACCTGCAGGTGTTTGCTATGTTCGCGTCT
GCCTACATGCTGGTGGTCATGACCGCGGACCGCTAC
ATCGCGGTGTGCCACCCGCTCAAGACCCTGCAG
CAGCCTGCGCGCCGCTCGCGCCTCATGATCGCTGCC
TCCTGGGTGTTGAGTTTCCTACTGAGCACGCCACAG
TACTTCATCTTCTCTATGATCGAAATCGAGGTGAAC
AACGGTACCAAAACTCAAGACTGCTGGGCTACCTTC
ATCCAGCCTTGGGGTCCCCGCGCCTACGTGACCTGG
ATGACCAGCGGTGTCTTTGTGGCACCTGTGATCGTC
TTGGGTACCTGCTATGGCTTCATCTGTTACCACATC
TGGAGCAATGTCCGCGGGAAGACGGTGTCGCGA
CAGAGCAAGGGCAGCAAGGGCTCTGGGGAAGCC
TTGGGTCCCTTCCACAAGGGGCTTCTGGTCACGCCT
TGTGTCAGCAGCGTGAAGACCATTTCCCGCGCCAAG
ATCCGCACAGTGAAGATGACCTTTGTCATCGTAACT
GCATACATCCTCTGCTGGACGCCTTTCTTCATCGTC
CAGATGTGGTCCGTCTGGGATGACGATTTCGCCTGG
ACCGATTCAGAAAATCCTTCCATAACCATCACCGCG
TTACTGGCCTCCTTGAACAGCTGCTGCAACCCGTGG
ATATACATGTTTTTTAGTGGCCACCTCCTGCAAGAC
TGTGTCCAAAGTTTGCCGTGCTGCCAAAGCGTGGCT
CAGAAATTCACCAAGGACGACTCAGACAGCATG
AGCCGAAGACAGACTTCGTACTCCAACAACCGA
AGCCCAACAAACAGCATCGGGACATGGAAGGAC
TCGCCTAAATCTTCCAAGTCCATCAGGTTCATTCCT
GCTTCCACCTGA.

Oxytocin receptor gene

ATGGAGGGCACGCCGGCAGCCAACTGGAGCATC
GAGTTGGACTTCGGGAGTGGAGTGCCACCAGGG

GTGGAGGGAAACCGCACAGCCGGTCCGCCAAGG
CGCAACGAGGCCCTGGCGCGGGTGGAGGTGGCG
GTGCTGTGCCTCATTCTGTTCCTGGCACTGAGCGGC
AACGCGTGCGTGCTGCTGGCTCTGCGCACCACG
CGCCACAAACATTCGCGTCTCTTCTTTTTCATGAAG
CACCTGAGCATCGCCGACTTGGTGGTGGCTGTGTTC
CAGGTGCTCCCGCAGCTGCTGTGGGACATCACCTTT
CGCTTCTACGGGCCCGACTTGCTGTGTCGTCTGGTC
AAATACTTGCAGGTGGTGGGCATGTTCGCCTCTACT
TACCTGTTGCTGCTCATGTCGCTCGACCGCTGCCTG
GCCATTTGCCAGCCTCTGCGTTCGCTGCGCCGCCGA
ACGGACCGCCTGGCGGTGCTGGCGACGTGGCTC
GGCTGCCTAGTGGCTAGCGCGCCGCAGGTGCAC
ATTTTCTCACTGCGCGAAGTGGCAGACGGCGTCTTT
GATTGCTGGGCGGTCTTCATCCAGCCCTGGGGACCC
AAGGCCTACGTCACGTGGATCACGCTTGCTGTCTAC
ATTGTGCCTGTCATCGTGCTGGCCGCCTGCTATGGC
CTCATCAGCTTCAAGATCTGGCAGAACCTGCGGCTC
AAGACGGCAGCAGCGGCTGCTGCAGCCGAGGGG
AGTGATGCCGGCGGAGGTGGGCGTGCGGCACTG
GCAAGGGTCAGTAGTGTCAAGCTCATCTCCAAG
GCCAAGATCCGCACAGTGAAGATGACCTTCATTATC
GTACTGGCCTTCATCGTCTGCTGGACGCCTTTCTTC
TTCGTGCAGATGTGGAGCGTCTGGGATGTCAATGCG
CCCAAGGAAGCGTCTGCCTTCATCATTGCCATGCTC
TTGGCCAGCCTCAACAGCTGCTGCAACCCCTGGATC
TACATGCTCTTCACAGGTCACCTCTTCCACGAACTT
GTGCAGCGCTTCCTCTGCTGCTCCGCCCGGTACCTG
AAGGGCAGTCGGCCCGGAGAAACAAGCATCAGC
AAGAAAAGCAACTCATCCACCTTTGTCCTGAGTCGT
CGCAGCTCCAGCCAGCGGAGCTGTTCTCAGCCATCC
TCAGTGTGA.

The full protocol was as follows. Tissue was fixed for 60 min at room temperature in 4% paraformaldehyde in 0.1 M phosphate buffer saline (PBS) and then rinsed twice in 0.1 M PBS. The tissue was then dehydrated in 50%, 70%, and two changes of 100% ethanol for 5 min each. Slides were air dried for 5 min before applying a hydrophobic barrier using an ImmEdge Hydrophobic Barrier Pen (Vector Laboratories, Burlingame, CA, USA). Each section was completely covered in hydrogen peroxide (600–1800 µL per slide) and incubated in the HybEZ Humidity Control Tray at room temperature for 10 min. Slides were washed twice in deionized water. Then, 300 µL of Protease III was pipetted on to each slide. Slides were incubated at room temperature in the HybEZ Humidity Control Tray for 5 min and then rinsed twice in 0.1 M PBS. Next, 300 µL of the appropriate probe mix was added to each slide. The experimental probe mix consisting of RNAscope Probe—Ad-Oxtr and RNAscope Probe—Ad-Avpr1a was added to the experimental slides. The probe mix for the positive control slide was RNAscope Probe—Mun-Polr2a and the probe mix for the negative control slide was RNAscope Probe—Mun-Ppib-C2.

In situ hybridization imaging and mRNA expression analysis

Slides were imaged using the Vectra Polaris slide scanner (Akoya) within one week of staining. An autofluorescence channel was captured during scanning. We measured the percentage of cells within a ROI that expressed mRNA using the Fluorescent RNAscope Image Analysis in QuPath protocol (technical note MK 51–154, Advanced Cell Diagnostics, Newark, CA, USA).

Briefly, slide scanner images were imported as fluorescent images into a project in QuPath (Bankhead et al. 2017). Each section was then "imaged" from these scanner images by drawing a rectangular annotation around the entirety of each section, sending the region to ImageJ, and saving the annotation as its own file. In doing so, each image was then small enough to be processed in FIJI. In FIJI, the background subtraction tool was used on each channel (DAPI, *Oxtr*, *Avpr1a*, and autofluorescence) with a rolling ball radius of 50. Then, the autofluorescence channel was subtracted from the *Oxtr* and *Avpr1a* channels to remove noise. This removed any objects that co-occurred in both the autofluorescence and signal channels and corrected the uneven autofluorescence between and across subjects.

ROIs identified during the autoradiography assay were assessed for mRNA expression. In QuPath, two annotations of equal size, one on the left hemisphere and one on the right, were placed on the ROI using the Specify Annotation function. Then, the Cell Detection module was used to segment cells within the annotation box stained with DAPI. The following parameter values were used: requested pixel size of 0.5 µm, background radius of 10 µm, median filer radius of 0 µm, sigma of 1.5 µm, minimum area of 10 μm^2, maximum area of 400 μm^2, and cell expansion of 5 µm. 'Split by shape', 'include cell nucleus', 'smooth boundaries', and 'make measurements' were all selected. To account for uneven DAPI staining, a unique threshold was determined for each image by measuring from ten background regions, consistent with the DEFiNE quantification method (Powell et al. 2019). The average mean and standard deviation across the ten measurements were calculated and the threshold was set at 4 standard deviations above the mean. In our dataset, this resulted in threshold values ranging from 3 to 28.

Once the cells were segmented, the Subcellular Detection Module was used to detect the fluorescently labeled probes within cell boundaries. The following parameter values were used: expected spot size of 2 μm^2, min spot size of 0.5 μm^2, and a maximum spot size of 6 μm^2, following the Technical Note's recommended settings. 'Include clusters' was selected. Like with the DAPI channel, a unique threshold was determined for each channel based on the average background. For *Oxtr* mRNA, a threshold ranging from 1 to

3 was applied and for *Avpr1a* mRNA, the thresholds ranged from 1 to 4.

Detection measurements were exported from QuPath into Excel for summarization. To minimize noise, a cell needed to have at least two puncta detected within its boundaries. Data were quantified to reflect the percentage of cells that express mRNA within a ROI. The sample size was too small to perform any statistical analyses and the subsequent results will be described qualitatively by binning each individual's results into the following ranges: 1–25% (+), 26–50% (++), 51–75% (+++), 76–100% (++++) (as described in Inoue et al. 2022).

Nissl staining procedure

The slides used for OXTR autoradiography were counter stained using toluidine blue Nissl. Briefly, slides were submerged in the dark in 180 mL of deionized water with 500 µL of 0.125 M toluidine blue stock solution. Then, the tissue was rinsed in deionized water and dehydrated in 70% ethanol for 20 s, 95% ethanol for 30 s, and two rinses of 100% ethanol for 3 min each. Then the slides were submerged in two rinses of Xylene for 5 min each. Slides were cover slipped using DPX. Slides were imaged using an Epson Perfection V700 photo scanner (Epson, Suwa, Nagano, Japan) in RGB mode at 2500 dpi.

Statistics

All statistical analyses were performed in SPSS 28 (IBM Analytics, USA). We were interested in characterizing sex differences in functional protein within regions of the SDMN and therefore analyzed tissue processed via receptor autoradiography. Data were normally distributed, and thus we compared receptor binding between sexes in brain regions in the SDMN when binding was present using independent samples *t* tests. The false discovery rate (FDR) procedure was used to correct for multiple comparisons, which were calculated separately for OXTR and AVPR1A. Corrected p values are reported in the figures. Both uncorrected and corrected p values are in Tables 1 and 2. Figures were made using Prism 9 (GraphPad, USA). We did not examine sex differences in mRNA expression due to limitations of RNAscope. The processing system (i.e., HybEZ™) can accommodate a maximum of 20 slides. With the need for control slides, this limits the number of experimental slides that can be processed in a single run. To process tissue for nearly whole brains and have a sample size sufficient to detect associations with gonadal sex, multiple runs would be needed. Because there can be substantial variation in mRNA labeling across runs, it would be difficult to disentangle associations with gonadal sex from effects of batch/run. Additional analyses described as follows were conducted in R version 4.0.5 (2021-03-31) (Team 2013). To visualize

Table 2 Statistical details of associations with gonadal sex for AVPR1A binding densities in regions of the Social Decision-Making Network of spiny mice

Brain region	T(df)	*p* value uncorrected	*p* value FDR corrected	Effect size (Cohen's *d*)
LS	T(14) = 1.02	0.33	0.66	1.30
VPall	T(13) = 2.01	0.06	0.26	0.48
MPOA	T(14) = 0.48	0.64	0.85	0.01
BNSTa	T(12) = 1.21	0.26	0.68	0.25
AH	T(14) = 2.47	0.03	0.23	0.14
MeA	T(14) = 0.56	0.59	0.94	0.47
VMH	T(14) = 0.01	0.99	0.99	0.85
PAG	T(14) = 0.18	0.86	0.98	0.10

Table 1 Statistical details of associations with gonadal sex for OXTR binding densities in regions of the Social Decision-Making Network of spiny mice

Brain region	*T*(df)	*p* value uncorrected	*p* value FDR corrected	Effect size (Cohen's) *d*	Direction of sex effect
NAcc	*T*(14) = 1.16	0.27	0.30	0.58	
LS	*T*(14) = 3.21	< 0.01	**0.02**	1.62	Higher in males
VPall	*T*(14) = 1.32	0.210	0.26	0.66	
MPOA	*T*(14) = 1.15	0.27	0.29	0.58	
BNSTa	*T*(14) = 5.78	< 0.01	**< 0.01**	2.91	Higher in males
BNSTp	*T*(14) = 7.29	< 0.01	**< 0.01**	3.65	Higher in males
AH	*T*(14) = 5.76	< 0.01	**0.01**	2.88	Higher in males
BLA	*T*(14) = 0.89	0.39	0.39	0.45	
MeA	*T*(14) = 1.96	0.07	0.11	0.98	
CPu	*T*(14) = 2.32	0.04	0.08	1.16	
VMH	*T*(14) = 1.68	0.12	0.17	0.84	
Hi	*T*(14) = 2.23	0.04	0.08	1.12	

Significant effects after correction for multiple comparisons are bolded

binding density patterns across brain regions, we used Pearson correlation matrices calculated via the R function "cor" to generate heatmaps via the function 'heatmap.2' in the R package 'gplots.' We then conducted hierarchical clustering analyses on the binding density data using the R package 'pvclust' (Suzuki et al. 2019) with distance metric set to 'correlation', linkage metric set to 'average', and bootstrap values set to 1000. Significant clusters were defined as those with an approximately unbiased (AU) p value > 95.

Results

Mapping of OXTR and AVPR1A binding in the basal forebrain and midbrain

To map expression of OXTR and AVPR1A binding in the brains of male and female spiny mice, we conducted receptor autoradiography on brain sections extending from the olfactory bulbs to the periaqueductal gray. We observed I-125 OVTA and I-125 LVA binding across several brain regions, namely olfactory areas, cortical areas, hippocampal areas, striatal areas, the pallidum, the amygdala, the hypothalamus, the thalamus, and the midbrain. Representative autoradiograms demonstrating receptor distributions are provided for OXTR in Fig. 2 and AVP1aR in Fig. 3.

Sex effects in brain regions involved in social behavior and reward

To determine if gonadal sex influences nonapeptide receptor densities as has been observed for other species (Dumais et al. 2013), we examined associations with gonadal sex on receptor binding in brain regions in the SDMN. We observed OXTR binding throughout more regions of the SDMN compared to AVPR1A binding. Additionally, independent t-tests revealed an association of gonadal sex on OXTR binding in the LS, BNST, and AH, with males having higher binding densities than females (all $p < 0.02$; Fig. 4A; Table 1). We previously found nonapeptide-producing neuronal sex differences in anatomy (Kelly and Seifert 2021) and function (Kelly unpub. obs) on an anterior–posterior axis of the BNST population of spiny mice, and therefore analyzed anterior and posterior portions of the region separately here. However, we observed similar findings for both compartments of the BNST. We found no associations with gonadal sex on any AVPR1A binding sites within the SDMN (all $p > 0.23$; Fig. 4B; Table 2).

Co-expression patterns of OXTR and AVPR1A binding in the SDMN

Because brain regions within the SDMN are anatomically interconnected and may coordinate activity to modulate distinct social behaviors (Deng et al. 2019; Dong and Swanson 2006; Newman 1999; O'Connell and Hofmann 2011), we ran correlational analyses for OXTR and AVPR1A binding for each sex to explore relationships between binding densities in these regions. To assess correlated OXTR and AVPR1A binding expression between pairs of regions, we first conducted Pearson correlation tests. The resulting correlation coefficients were visualized using a heatmap; due to the exploratory nature of the analysis, we did not correct for multiple comparisons. While males showed a mix of positive

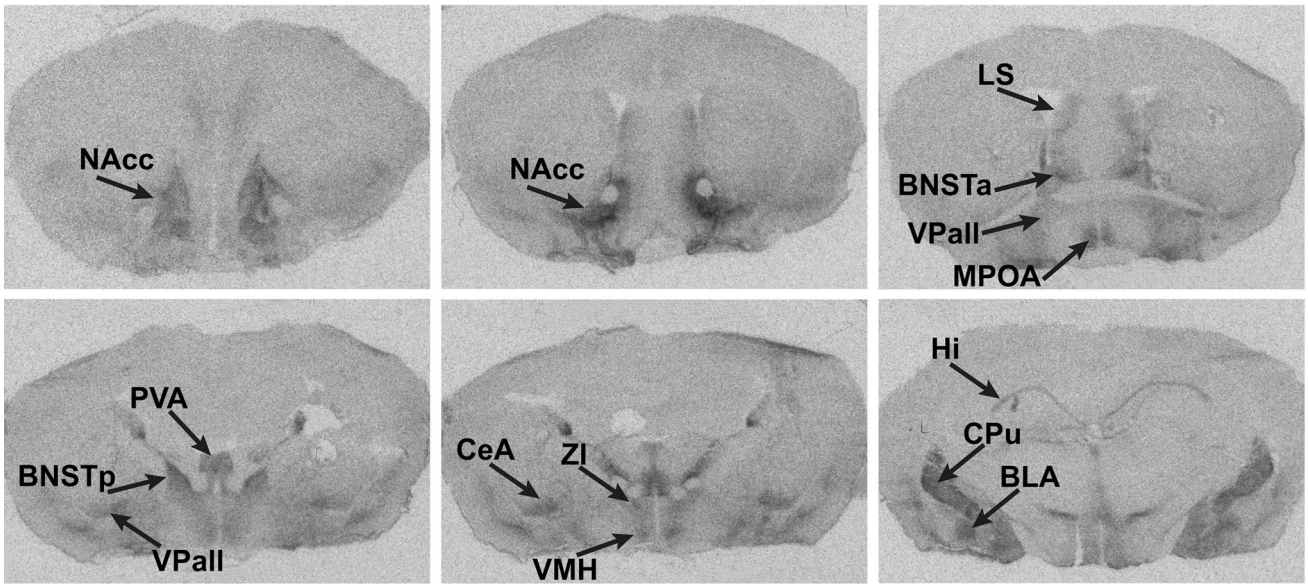

Fig. 2 OXTR binding. Representative autoradiograms of OXTR binding in coronal sections from spiny mouse tissue

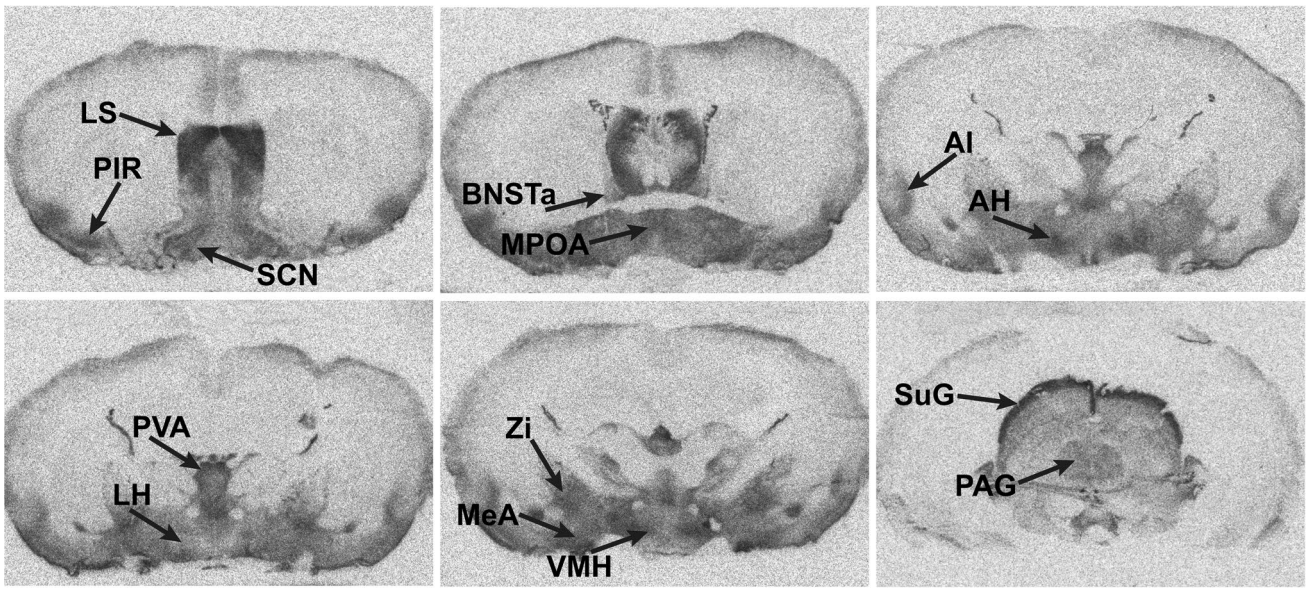

Fig. 3 AVPR1A binding. Representative autoradiograms of AVPR1A binding in coronal sections from spiny mouse tissue

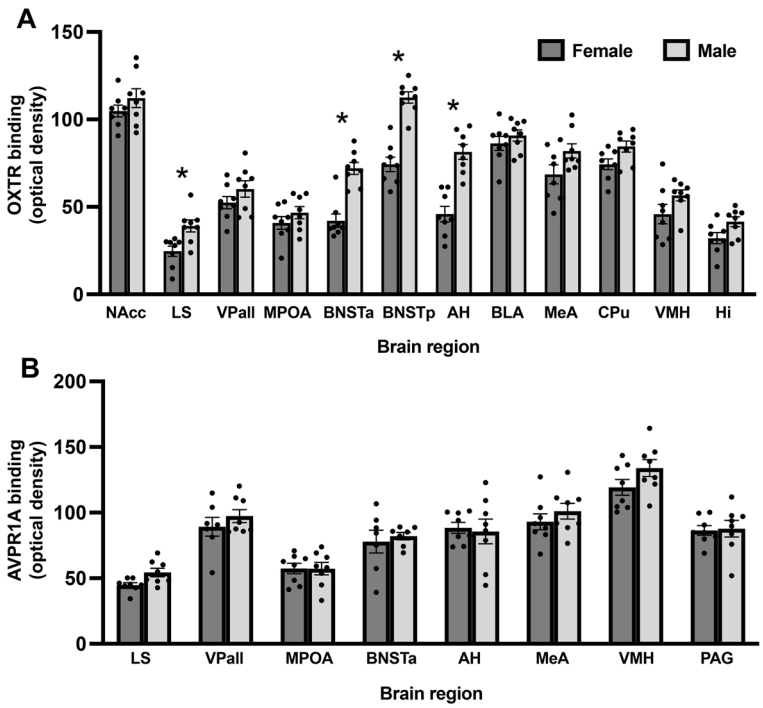

Fig. 4 Associations with gonadal sex on OXTR and AVPR1A binding. Mean grayscale values (± SEM) for **A** OXTR and **B** AVPR1A binding in brain regions of the Social Decision-Making Network (SDMN) in male and female spiny mice. *Denotes $p_{corrected} < 0.05$

and negative correlations in OXTR binding between brain regions across the SDMN, females showed primarily positive correlations (Fig. 5A). However, the opposite pattern emerged for AVPR1A binding (Fig. 5B).

To further explore patterns of co-expression across SDMN regions, we performed hierarchical clustering analyses using the R package 'pvclust' (Suzuki et al. 2019) with distance metric set to 'correlation', linkage metric set to 'average', and bootstrap values set to 1000. Significant clusters were defined as those with an approximately unbiased (AU) p value > 95. Again, the two sexes exhibited distinct co-expression patterns. For OXTR binding in male spiny mice, hierarchical clustering identified a large cluster comprised of the NAcc, MeA, BNSTp, VPall, BLA, LS, CPu, BNSTa, and Hi, whereas in females we observed a large cluster consisting of the BNSTa, BNSTp, VMH, VPall, BLA, and Hi, as well as a small cluster comprised of the MeA and AH (Fig. 5A). Despite observing

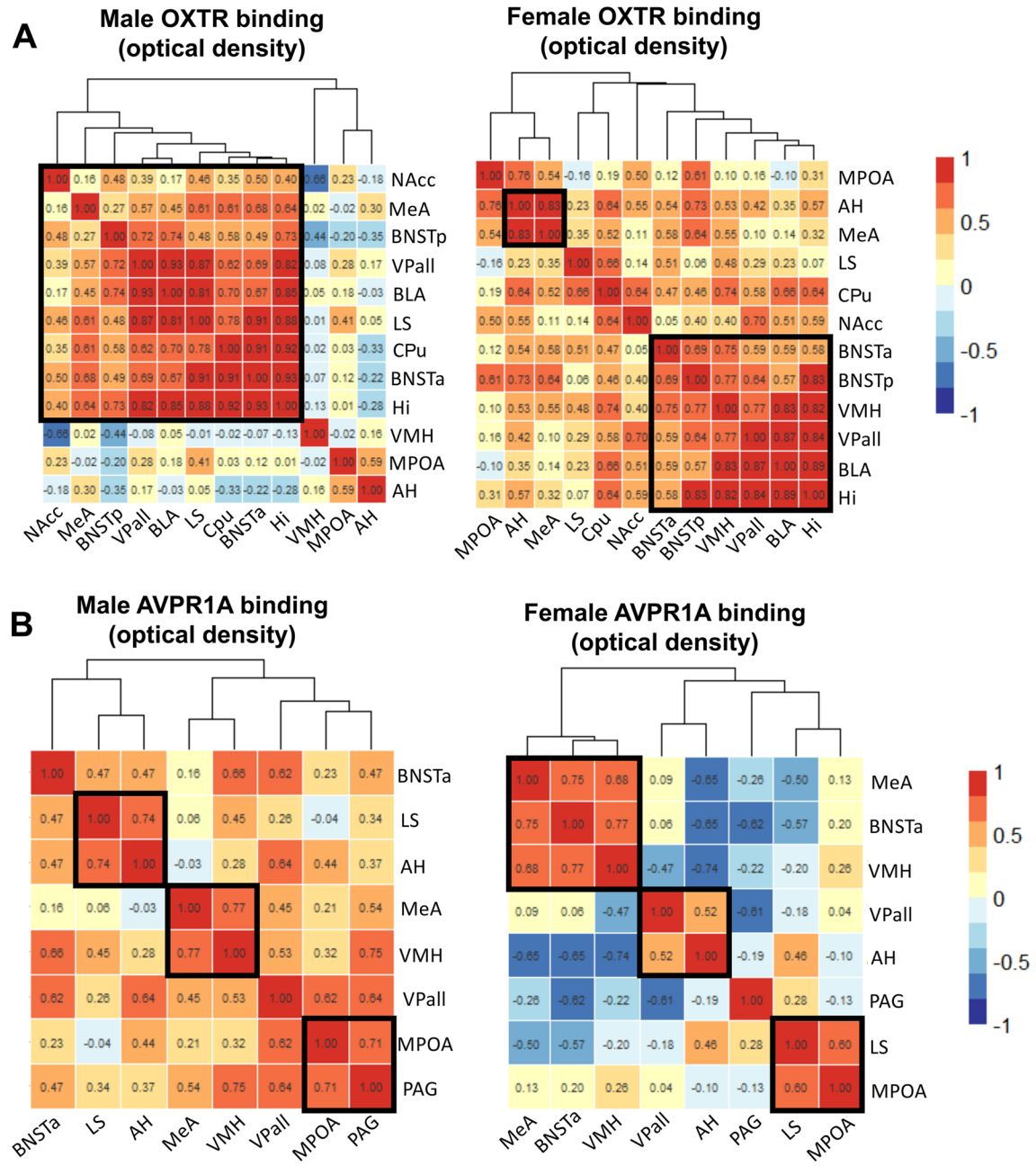

Fig. 5 Pairwise comparisons and hierarchical clustering of **A** OXTR and **B** AVPR1A binding expression across regions of the SDMN. Values shown are Pearson correlation coefficients. Significant cluster (AU > 95) are outlined in black boxes. Due to small sample sizes, note that this is exploratory in nature

no sex differences in AVPR1A binding in individual brain regions, the co-expression patterns for AVPR1A binding across the SDMN are strikingly different for males and females. Hierarchical clustering revealed 3 clusters for males: (1) LS and AH, (2) MeA and VMH, and (3) MPOA and PAG, and 3 clusters for females: (1) MeA, BNSTa, and VMH, (2) VPall and AH, and (3) LS an MPOA (Fig. 5B).

Mapping of Oxtr and Avpr1a mRNA in the basal forebrain and midbrain

To investigate expression of *Oxtr* and *Avpr1a* mRNA in the spiny mouse brain, we performed RNAscope in situ hybridization in 2 male and 2 female brains on sections extending from the olfactory bulb through the periaqueductal gray. We

Table 3 *Oxtr* and *Avpr1a mRNA* expression across the forebrain and midbrain of the spiny mouse

Region	*Oxtr* mRNA			*Avpr1a* mRNA			*n*
	Bins	Mean (%)	SD	Bins	Mean (%)	SD	
Olfactory areas							
AOB	+/++	10.99	10.99	+++/++++	79.28	9.56	4
AOA	+/+++	51.40	22.76	+/+++	26.38	24.69	4
MOBgl	+/++	20.06	8.31	+/++/+++	35.25	17.85	3
MOBgr	+/++	25.11	2.72	+/++	28.14	19.07	3
PIR	+	13.70	9.36	+	12.49	7.72	4
TT	+/++/+++	38.68	20.71	+/+++	39.38	22.60	4
Cortex							
AI	+/++	18.47	21.33	+/++/+++	28.76	19.59	4
Cg2	+/+++	22.88	21.29	+/++	28.69	13.20	4
Cg5	+/++/+++	36.97	19.04	+/++	21.63	12.54	4
DI	+/+++	28.08	22.64	+/+++	21.11	21.01	4
Striatum							
CPu	+/++	31.04	7.15	+	7.89	5.76	4
LS	+	8.22	5.01	+++	59.35	6.85	4
NAcc	++	38.41	6.17	+/++	17.65	16.55	4
OT	+/++	18.68	19.40	+/++	21.92	16.21	4
Pallidum							
BNSTa	+/++/+++	31.52	19.39	+/++	13.63	9.41	4
BNSTp	+/++/+++	39.56	22.22	+/++	13.17	13.52	4
VDB	+	7.02	1.79	+	13.24	3.16	4
GP	+/++	21.11	14.62	+/++	23.61	18.97	4
VP	+/++	17.94	10.71	+	15.58	9.08	4
Hypothalamus							
AH	+/++	20.56	12.35	+/++	27.84	10.90	4
LH	+	16.25	5.24	+/++	16.88	11.70	4
MM	+	11.91	7.74	+	13.85	4.49	4
MPOA	+/++	9.71	13.19	+/++	21.64	13.53	4
VMH	+/++	19.01	11.02	+	16.53	7.04	4
ZI	+/++	21.31	17.79	+	9.50	5.29	4
Thalamus							
LD	+/++	11.02	10.43	+	11.96	8.03	4
MG	+/++	9.95	13.42	+/++	17.85	13.31	4
PVA	+	14.68	8.40	+/+++	51.16	29.04	4
PVG	+	15.70	8.22	+/++	25.38	17.55	4
Re	+	10.59	6.72	+/++	36.01	17.31	4
VPL	+/+++	18.40	23.42	+/++	13.41	12.40	4
Amygdala							
AHAL	+/+++/++++	45.49	38.16	+	11.86	10.48	4
BLA	+/++	32.58	10.25	+/++	15.84	10.39	4
CeA	++/+++	40.49	10.80	+	11.89	6.63	4
MeA	+/++	19.18	11.36	+	12.41	5.12	4
Hippocampus							
CA1py	+/++	7.68	12.13	+	4.75	4.62	4
Midbrain							
APT	+/++	13.97	20.29	+/++	22.96	20.05	4
IP	+	2.84	1.65	+/++/+++	39.88	15.20	4
PAG	+	6.65	3.79	+/++	11.55	11.95	4
PVG	+	15.70	8.22	+/++	25.38	17.55	4

Table 3 (continued)

Region	*Oxtr* mRNA			*Avpr1a* mRNA			*n*
	Bins	Mean (%)	SD	Bins	Mean (%)	SD	
SuG	+	6.11	6.54	+	15.34	12.35	4
SCm	+	7.41	9.68	+/++	8.80	6.78	4

Oxtr and *avpr1a* were labeled in the brain using duplex in situ hybridization, and the percentage of *Oxtr*+ and *Avpr1a*+ cells were calculated for each ROI. The data were binned into the following categories based on the percentage of cells expressing mRNA: +: ≤ 25%; ++: 25% < × ≤ 50%; +++: 50% < × ≤ 75%; ++++: > 75%

Multiple bins reflect variability across subjects. Mean and standard deviations represent the percentage of cells that were positive for the relevant transcript

observed both *Oxtr* and *Avpr1a* mRNA in 42 brain regions (see Table 3 for qualitative results). Nonapeptide receptor mRNA expression was observed in all regions of both sexes. Particularly robust *Oxtr* labeling was observed in the NAcc, BNST, and AH (Fig. 6) and robust *Avpr1a* labeling was observed in the LS, MPOA, and Hi (Fig. 7). Unlike OXTR and AVPR1A binding, all brain regions within the SDMN expressed some *Oxtr* and *Avpr1a* mRNA. For example, we observed *Oxtr* mRNA, but no OXTR binding, in the PAG. Further, we observed *Avpr1a* mRNA, but no AVPR1A binding, in the NAcc, CPu, BLA, and Hi. This suggests that nonapeptide receptors may be synthesized in these regions but transported to other areas of the brain.

Discussion

Here we provide the first characterization of distributions of OXTR and AVPR1A binding and *Oxtr* and *Avpr1a* mRNA in the basal forebrain and midbrain of the adult spiny mouse. We examined the effect of sex on functional protein throughout brain regions of the SDMN, and found that OXTR binding densities in the LS, BNSTa, BNSTp, and AH were greater in males compared to females. However, we observed no associations with gonadal sex in AVPR1A binding in individual brain regions. Interestingly, exploratory correlational analyses and hierarchical clustering revealed distinct patterns of AVPR1A and OXTR co-expression for males and females, suggesting that nonapeptide receptors in neuroanatomically connected regions may differentially coordinate activity in male and female spiny mice.

Similarities and dissimilarities in SDMN OXTR and AVPR1A binding in spiny mice and other rodents

There is an extraordinary amount of variation in nonapeptide receptor distributions and densities across species (Beery et al. 2008; Olazabal and Sandberg 2020; Froemke and Young 2021). Although we characterized nonapeptide receptor binding and mRNA distributions throughout the basal forebrain and midbrain of spiny mice, we focused analyses on regions within the SDMN. The SDMN comprises brain regions involved in multiple types of social behavior as well as those in the mesolimbic reward system (O'Connell and Hofmann 2011, 2012). The hypothesis of SDMN function is that the network evaluates the salience of stimuli to facilitate a context-appropriate behavioral response, thus allowing an animal to cope with challenges and take advantage of opportunities in an ever-changing social environment. The presence of nonapeptide receptors in SDMN regions has been reported for several rodents, with more extensive characterizations in prairie voles and Wistar rats (Prounis et al. 2018; Smith et al. 2017).

We observed OXTR and AVPR1A binding throughout most regions of the SDMN in male and female spiny mice. Notably, we did not detect OXTR binding in the PAG or AVPR1A binding in the BLA, CPu, Hi, and NAcc. Few studies have assessed OXTRs in the PAG, however, the lack of OXTR binding in the PAG of spiny mice is consistent with what has been reported for Wistar rats (Smith et al. 2017). Similarly, an absence of AVPR1A binding in the BLA and CPu has also been reported for prairie voles and Wistar rats (Prounis et al. 2018; Smith et al. 2017). While AVPR1A binding is largely absent in the Hi of prairie voles and Wistar rats (Prounis et al. 2018; Smith et al. 2017), the dentate gyrus (DG) of the Hi typically shows robust OXTR binding in rats and tuco-tucos (Beery et al. 2008; Smith et al. 2017); yet, we observed no AVPR1A binding in the Hi or DG of spiny mice. Although, like spiny mice, AVPR1A binding in the NAcc is largely absent in prairie voles (Prounis et al. 2018), AVPR1A binding is present in a small portion of the shell of the NAcc in Wistar rats (Smith et al. 2017). Conversely, we observed moderate OXTR binding in the NAcc of spiny mice. The OXTR population of the NAcc is arguably one of the most well-studied nonapeptide receptor sites and exhibits a great deal of variation in binding densities even within a species. NAcc OXTR distinguishes mating system in monogamous and non-monogamous voles, relates to alloparental care and pairbond formation in prairie voles, regulates various aspects of social bonding and alloparental behavior in voles, and facilitates social reward

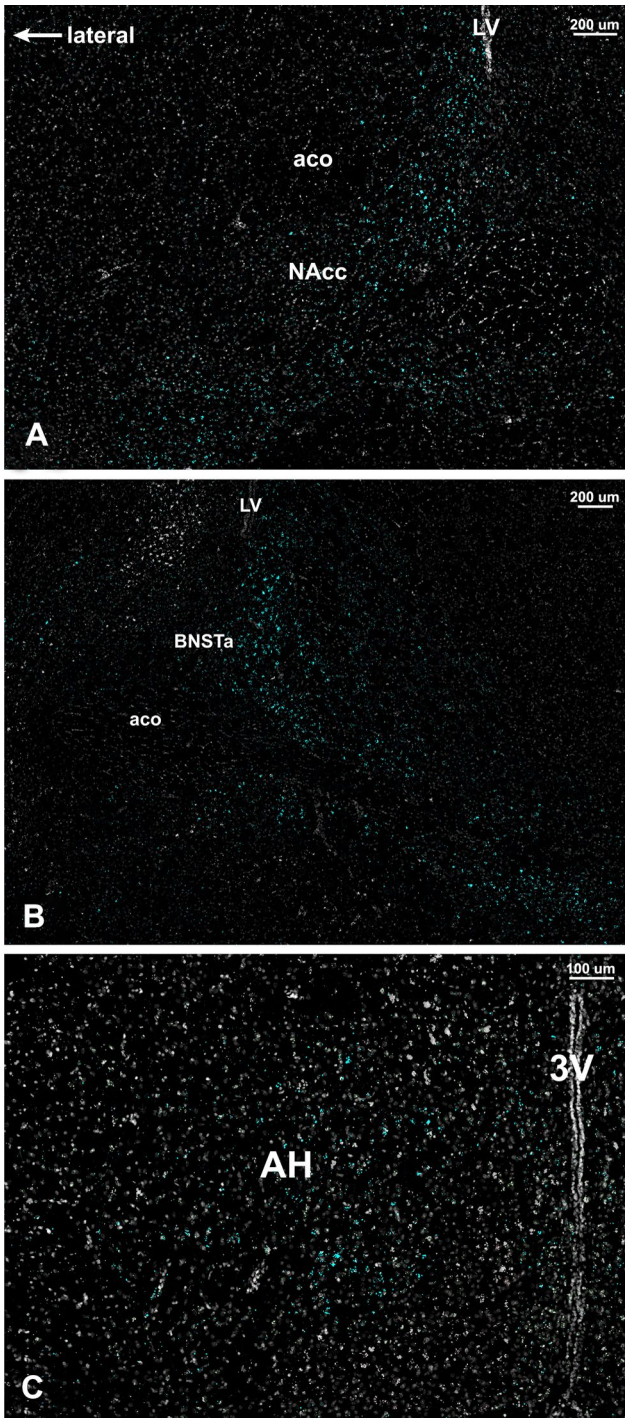

Fig. 6 *Oxtr mRNA expression in the spiny mouse.* Representative images of *Oxtr* mRNA expression from a female spiny mouse brain in the **A** NAcc **B** BNSTa, and **C** AH

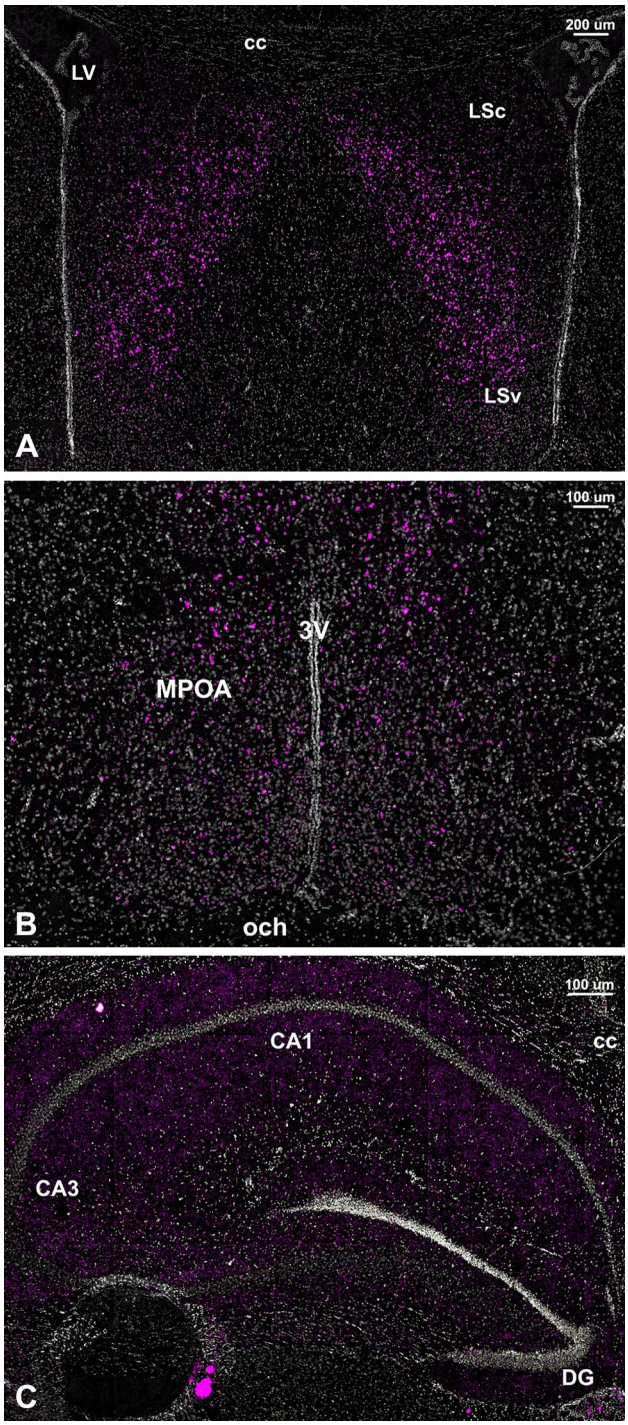

Fig. 7 *Avpr1a mRNA expression in the spiny mouse.* Representative images of *Avp1ra* mRNA expression from a female spiny mouse brain in the **A** LS, **B** MPOA, and **C** Hi

processing in C57/BL6 mice (Dolen et al. 2013; Liu and Wang 2003; Borie et al. 2022a; Bosch et al. 2016; Keebaugh et al. 2015; Barrett et al. 2015). Interestingly, the spiny mice showed a unique expression pattern compared to other species such that OXTR binding was largely restricted to the shell. Previous research has shown that the NAcc core and shell can differentially influence behaviors such as reward- and drug-seeking and learning (Chaudhri et al. 2010; Ito and Hayen 2011; Rossi et al. 2020); together these studies support a role for the NAcc shell in mediating the influence

of contexts on behavior. Given that spiny mice live in large groups and experience a wider range of social interactions than species that are solitary or live in small family groups, OXTRs in the NAcc shell of spiny mice may play a large role in distinguishing social context, thus facilitating context-appropriate responses to a dynamic social environment.

Interestingly, to our knowledge, OXTR binding has not been reported in the AH of rodents (but see the presence of *Oxtr* mRNA in the AH of prairie voles (Inoue et al. 2022)), however, we observed moderate OXTR binding in the AH of spiny mice, with higher binding densities in males. This finding mirrors a previous observation in spiny mice, such that they express an especially robust AH OXT neuronal population, which overlaps with the evolutionarily conserved AH AVP cell group (Kelly and Seifert 2021). Few studies have examined the role of OXT or OXTRs in the AH, however, a study that injected OXT into the "MPO-AH continuum" found a decrease in aggression in female hamsters, suggesting that AH OXT may have anti-aggressive functional properties (Harmon et al. 2002); because OXT and AVP promiscuously bind to both OXTRs and AVPR1As (Leung et al. 2009; Liu et al. 2001; Taylor et al. 2020), whether this effect is the result of OXT acting on OXTRs or AVPR1As remains unclear. An interesting consideration for future studies is to examine the role of, and potential functional sex differences in, AH OXTRs in spiny mice. It is feasible that the higher densities of OXT-immunoreactive (ir) neurons and OXTRs in the AH may serve to promote the highly prosocial and low aggressive phenotype of the spiny mice.

Species-typical group size and OXTR binding in the lateral septum

In a recent review examining OXTR binding densities in the LS across rodents that range in social group size, Olazabal and Sandberg identified that LS OXTR binding densities are lower in species that have low conspecific spacing, live in medium to large groups, and exhibit low levels of aggression compared to species that have high conspecific spacing, live in small to medium groups, and exhibit higher degrees of aggression (Olazabal and Sandberg 2020). Spiny mice fit this pattern and like colonial tuco-tucos, Norway rats, short-tailed singing mice, and guinea pigs, LS OXTR binding is relatively light in the spiny mouse brain (Beery et al. 2008; Campbell et al. 2009; Tribollet et al. 1992b, 1992a). Similar to these rodents, spiny mice also live in large communal groups and display low levels of aggression (Deacon 2009; Fricker et al. 2021; Frynta et al. 2011; Nowak 1999). Perhaps not surprisingly, this pattern does not hold true for all rodents, though. Large group-living eusocial naked mole rats and their solitary relative do not show detectable levels of OXTRs in the LS (Kalamatianos et al. 2010). Furthermore, LS OXTR binding patterns show an opposite pattern for Estrildid finches, such that more gregarious species that live in large groups show higher septal OXTR binding densities compared to territorial, solitary finch species (Goodson et al. 2009).

While it may be somewhat informative to search for a reflection of social phenotypes within single brain regions, it is more likely that broad social phenotypes reflect diverse patterning of nonapeptide receptors, as well as other neural systems, across the brain. Indeed, species-typical group size is associated with an array of social behaviors that vary within and across species. Although some large group-living species are communal breeders and readily care for unrelated young (i.e., spiny mice), other species remain socially monogamous within large groups and care only for their own offspring or kin (i.e., zebra finches) (Tuckova et al. 2016; Zann 1996). Additionally, behaviors such as alloparental care are observed in both small and large group-living species (Kenkel et al. 2017; Tuckova et al. 2016). Along these lines, a recent meta-analysis determined that OXTR and AVPR1A binding distributions are more consistent within than across genera in rodents, suggesting that a within-genus comparison of nonapeptide receptor distributions is more appropriate than comparing across distant species (Freeman et al. 2020). This provides support for the hypothesis that distinct evolutionary selective pressures act on nonapeptide receptor patterning [in Rodentia], leading to differential receptor binding patterning across species while also urging caution when seeking to generalize nonapeptide receptor anatomy or function across species not within the same genus.

Associations with gonadal sex on OXTR and AVPR1A binding densities within the SDMN

Here we found that male spiny mice exhibited higher densities of OXTR binding in the LS, BNST, and AH compared to females. Widespread sex differences in OXTR binding have been reported for Wistar rats, again with males exhibiting greater OXTR binding densities than females (Smith et al. 2017). Similar to spiny mice, male California mice and deer mice also show more OXTR binding in the LS and BNST than females (Insel et al. 1991). However, an absence of a sex difference in LS and BNST OXTR binding has been reported for prairie voles (Bales et al. 2007). Together, this highlights that variation in nonapeptide receptor densities is not only species-specific, but also sex-specific, and that findings in one species and/or sex should not necessarily be generalized to other species and/or sexes (Dumais et al. 2013).

To explore whether nonapeptide receptor binding co-expression patterns in the SDMN differ in male and female spiny mice, we conducted Pearson correlation tests followed by hierarchical clustering analyses. Note that our sample sizes were small for this analysis and that results and

interpretations are purely exploratory in nature. We observed different correlational patterns in males and females for both OXTR and AVPR1A binding, and although only exploratory, these analyses may suggest that more strongly correlated binding densities in brain regions or clusters of brain regions could underlie sex-specific behaviors. Despite a different appearance in clustering between the sexes, examining brain region relationships for individual SDMN nodes reveals some similarities between males and females. For example, OXTR binding in the Hi correlated strongly with several other brain regions in both males and females, suggesting that OXTRs in the Hi may be heavily functionally integrated in nonapeptide-mediated behavior, but not necessarily in a sex-specific manner. However, while male OXTR binding in the BNSTa correlated with binding in 3 other brain regions (LS, CPu, and Hi), BNSTa OXTR binding in females did not correlate with binding in other regions. A previous study found that BNSTa OXTR receptors promote stress-induced social avoidance in female, but not male, California mice (Duque-Wilckens et al. 2018). Together, these findings suggest that BNSTa OXTRs may coordinate activity with distinct brain regions in males and females and potentially mediate sex differences in behavior in the spiny mice. While both male and female spiny mice are socially bold and readily approach all types of conspecifics (Fricker et al. 2021), in our colony we have found that males are interactive with more individuals in a group than females and that females are more likely to exhibit aggression than males (Kelly et al. unpub obs). Given that BNSTa OXTRs in California mice promote social avoidance, similar functions may exist in female spiny mice, albeit to a different degree given the different life history and highly prosocial phenotype of the species.

The sex differences in OXTR binding reported here are consistent with our previous finding of widespread sex differences in OXT neuronal populations in the spiny mice. Males exhibited more OXT-ir neurons than females in the median preoptic nucleus, periventricular nucleus of the hypothalamus, BNST, lateral hypothalamus, and AH (Kelly and Seifert 2021). Because OXT generally promotes prosocial behaviors (Froemke and Young 2021; Goodson and Thompson 2010), future studies can seek to determine whether male spiny mice evolved a more robust OXT system to compensate for male aggression, thus promoting the prosociality needed for a communal breeding system to be successful. Indeed, sex differences in the brain do not always necessarily facilitate a sex difference in behavior, but may at times serve to prevent overt sex differences in behavior (De Vries 2004).

Although we observed no associations with gonadal sex on AVPR1A binding in brain regions throughout the SDMN, we did observe different co-expression patterns in AVPR1A binding between male and female spiny mice. Not only did we find more negative correlations in AVPR1A binding between brain regions in females than males, but the hierarchical clustering loaded 3 distinct clusters for the sexes. The most similar cluster in males and females was the MeA and VMH cluster in males and MeA, VMH, and BNSTa cluster in females. The MeA and VMH are brain regions important for the expression of defensive behaviors, aggression, and avoidance (Hashikawa et al. 2017; Hong et al. 2014; Li et al. 2017; Lin et al. 2011; Tong et al. 2020). It is intriguing that BNSTa also loaded onto this cluster in females, but not males, given that BNSTa OXTRs facilitate social avoidance in female, but not male California mice (Duque-Wilckens et al. 2020). Perhaps BNSTa AVPR1As are also involved in defensive and/or anti-social behaviors in spiny mice and play a more prominent role in facilitating those behaviors in females.

Presence of nonapeptide receptor mRNA but an absence of binding

Oxtr and *Avpr1a* mRNA was identified in 42 brain regions throughout the forebrain and midbrain of spiny mice. However, OXTR and AVPR1A binding were not observed in all sites of mRNA labeling. Within the SDMN, we observed the presence of nonapeptide receptor mRNA, but absence of binding for OXTR in the PAG and for AVPR1A in the NAcc, BLA, CPu, and Hi. This is consistent with a recent characterization of *Oxtr* mRNA distributions in the prairie vole, in which a misalignment in OXT receptor mRNA expression and binding was observed in some areas of the brain (Inoue et al. 2022). Such findings suggest that nonapeptide receptors may be synthesized in a region, but the receptor protein is transported to a distal site. Axonal transport of receptor protein to neighboring brain areas can enable presynaptic signaling (Dolen et al. 2013; Yoshimura et al. 1993). Additionally, transported receptor protein may be held in latent pools within neurons until trafficked to the membrane under particular conditions (Sheng and Cai 2012). Together, this generates greater plasticity in nonapeptide system functioning and provides more avenues in which other neural systems can act upon the nonapeptide system.

A note about Manning Compound for future studies in spiny mice

In our competitive binding assay, Manning Compound did not fully block I-125 LVA binding. This suggests that either Manning Compound has a lower binding affinity in the spiny mouse compared to other species or that I-125 LVA binds to additional proteins beyond AVPR1A. Because mRNA was expressed in all regions in which receptor binding was observed, it is likely that Manning Compound has a lower binding affinity in the spiny mouse

compared to other species. This is consistent with recent findings in the Syrian hamster where Manning Compound was found to not meet criteria for selectivity for AVPR1A (Taylor et al. 2020). Therefore, caution should be taken when considering experimental designs in spiny mice that intend to use Manning Compound for pharmacological manipulation.

Conclusion

Here we characterized the distributions of OXTR and AVPR1A binding, as well as *Oxtr* and *Avpr1a* mRNA expression, throughout the basal forebrain and midbrain of male and female spiny mice. We identified an effect of sex on OXTR, but not AVPR1A, binding, in several brain regions involved in social behavior. In all regions in which a sex difference was observed, males exhibited higher binding densities compared to females. Furthermore, via clustering analyses, we identified distinct patterns of OXTR and AVPR1A binding co-expression across SDMN brain regions for males and females. These data can inform future work in spiny mice that seek to examine sex differences in nonapeptide-mediated behavior. Together, these results lay a basic foundation for future studies that seek to manipulate nonapeptide receptors or nonapeptide neural circuits (i.e., connecting peptide-producing neuronal populations with downstream receptor sites) in spiny mice, thus providing a model that is ideal for exploring nonapeptide-mediated grouping behaviors.

Author contributions JMP cryosectioned brains, conducted in situ hybridization, quantified receptor binding and mRNA expression, and wrote the manuscript. KI conducted the competitive binding assays and receptor autoradiography. KJW analyzed the data. AWS provided feedback on and edited the manuscript. LJY designed the study, provided feedback on and edited the manuscript, and acquired funding. AMK designed the study, analyzed the data, wrote the manuscript, and acquired funding.

Funding We would like to acknowledge funding from the Esther A. and Joseph Klingenstein Fund (Klingenstein-Simons Fellowship Award in Neuroscience to AMK), the National Institute of Arthritis and Musculoskeletal and Skin Diseases (R01AR070313 to AWS), the National Science Foundation (IOS-1353713 to AWS), and the National Institute of Mental Health (Emory CONTE Center Pilot Project Grant; P50MH100023 to LJY and P51OD11132 to Emory National Primate Research Center).

Data availability Data are available upon request from the corresponding author.

Declarations

Competing interests The authors have no relevant financial or non-financial interests to disclose.

Ethics approval All procedures were approved by the Institutional Animal Care and Use Committee of Emory University.

References

Albers HE (2012) The regulation of social recognition, social communication and aggression: vasopressin in the social behavior neural network. Horm Behav 61(3):283–292. https://doi.org/10.1016/j.yhbeh.2011.10.007

Albers HE (2015) Species, sex and individual differences in the vasotocin/vasopressin system: relationship to neurochemical signaling in the social behavior neural network. Front Neuroendocrinol 36:49–71. https://doi.org/10.1016/j.yfrne.2014.07.001

Bales KL, Plotsky PM, Young LJ, Lim MM, Grotte N, Ferrer E, Carter CS (2007) Neonatal oxytocin manipulations have long-lasting, sexually dimorphic effects on vasopressin receptors. Neuroscience 144 (1):38-45. S0306-4522(06)01235-8 https://doi.org/10.1016/j.neuroscience.2006.09.009

Bankhead PP, Loughrey MB, Frenandez JA, Dombrowski Y, McArt DG, Dunne PD, McQuaid S, Gray RT, Murray LJ, Coleman HG, James JA, Salto-Tellez M, Hamilton PW (2017) QuPath: open source software for digital pathology image analysis. Sci Rep 7(1):16878. https://doi.org/10.1038/s41598-017-17204-5

Barrett CE, Keebaugh AC, Ahern TH, Bass CE, Terwilliger EF, Young LJ (2013) Variation in vasopressin receptor (Avpr1a) expression creates diversity in behaviors related to monogamy in prairie voles. Horm Behav 63(3):518–526. https://doi.org/10.1016/j.yhbeh.2013.01.005

Barrett CE, Arambula SE, Young LJ (2015) The oxytocin system promotes resilience to the effects of neonatal isolation on adult social attachment in female prairie voles. Transl Psychiatry 5:e606. https://doi.org/10.1038/tp.2015.73

Beery AK, Lacey EA, Francis DD (2008) Oxytocin and vasopressin receptor distributions in a solitary and a social species of tuco-tuco (Ctenomys haigi and Ctenomys sociabilis). J Comp Neurol 507(6):1847–1859. https://doi.org/10.1002/cne.21638

Bellofiore N, Ellery SJ, Mamrot J, Walker DW, Temple-Smith P, Dickinson H (2017) First evidence of a menstruating rodent: the spiny mouse (Acomys cahirinus). Am J Obstet Gynecol 216 (1):40 e41–40 e11. https://doi.org/10.1016/j.ajog.2016.07.041

Bellofiore N, Rana S, Dickinson H, Temple-Smith P, Evans J (2018) Characterization of human-like menstruation in the spiny mouse: comparative studies with the human and induced mouse model. Hum Reprod 33(9):1715–1726. https://doi.org/10.1093/humrep/dey247

Bester-Meredith JK, Young LJ, Marler CA (1999) Species differences in paternal behavior and aggression in *Peromyscus* and their associations with vasopressin immunoreactivity and receptors. Horm Behav 36(1):25–38. https://doi.org/10.1006/hbeh.1999.1522

Borie AM, Agezo S, Lunsford P, Boender AJ, Guo JD, Zhu H, Berman GJ, Young LJ, Liu RC (2022a) Social experience alters oxytocinergic modulation in the nucleus accumbens of female prairie voles. Curr Biol 32 (5):1026–1037 e1024. https://doi.org/10.1016/j.cub.2022a.01.014

Borie AM, Young LJ, Liu RC (2022b) Sex-specific and social experience-dependent oxytocin-endocannabinoid interactions in the nucleus accumbens: implications for social behaviour. Philos Trans R Soc Lond B Biol Sci 377(1858):20210057. https://doi.org/10.1098/rstb.2021.0057

Bosch OJ, Dabrowska J, Modi ME, Johnson ZV, Keebaugh AC, Barrett CE, Ahern TH, Guo J, Grinevich V, Rainnie DG, Neumann ID, Young LJ (2016) Oxytocin in the nucleus accumbens shell

reverses CRFR2-evoked passive stress-coping after partner loss in monogamous male prairie voles. Psychoneuroendocrinol 64:66–78. https://doi.org/10.1016/j.psyneuen.2015.11.011
Brunjes PC (1990) The precocial mouse, Acomys cahirinus. Psychobiology 18(3):339–350
Caldwell HK (2017) Oxytocin and vasopressin: powerful regulators of social behavior. Neuroscientist 23(5):517–528. https://doi.org/10.1177/1073858417708284
Campbell P, Ophir AG, Phelps SM (2009) Central vasopressin and oxytocin receptor distributions in two species of singing mice. J Comp Neurol 516(4):321–333. https://doi.org/10.1002/cne.22116
Chappell AR, Freeman SM, Lin YK, LaPrairie JL, Inoue K, Young LJ, Hayes LD (2016) Distributions of oxytocin and vasopressin 1a receptors in the Taiwan vole and their role in social monogamy. J Zool 299(2):106–115. https://doi.org/10.1111/jzo.12332
Chaudhri N, Sahuque LL, Schairer WW, Janak PH (2010) Separable roles of the nucleus accumbens core and shell in context- and cue-induced alcohol-seeking. Neuropsychopharmacology 35(3):783–791. https://doi.org/10.1038/npp.2009.187
Cizkova B, Sumbera R, Frynta D (2011) A new member or an intruder: how do Sinai spiny mouse (*Acomys dimidiatus*) families respond to a male newcomer? Behaviour 148(8):889–908
De Vries GJ (2004) Minireview: Sex differences in adult and developing brains: compensation, compensation, compensation. Endocrinology 145(3):1063–1068. https://doi.org/10.1210/en.2003-1504
Deacon RM (2009) Burrowing: a sensitive behavioural assay, tested in 5 species of laboratory rodents. Behav Brain Res 200:128–133
Deng K, Yang L, Xie J, Tang H, Wu GS, Luo HR (2019) Whole-brain mapping of projection from mouse lateral septal nucleus. Biol Open. https://doi.org/10.1242/bio.043554
Dolen G, Darvishzadeh A, Huang KW, Malenka RC (2013) Social reward requires coordinated activity of nucleus accumbens oxytocin and serotonin. Nature 501(7466):179–184. https://doi.org/10.1038/nature12518
Donaldson ZR, Young LJ (2008) Oxytocin, vasopressin, and the neurogenetics of sociality. Science 322(5903):900–904. https://doi.org/10.1126/science.1158668
Dong HW, Swanson LW (2006) Projections from bed nuclei of the stria terminalis, anteromedial area: cerebral hemisphere integration of neuroendocrine, autonomic, and behavioral aspects of energy balance. J Comp Neurol 494(1):142–178. https://doi.org/10.1002/cne.20788
Dumais KM, Bredewold R, Mayer TE, Veenema AH (2013) Sex differences in oxytocin receptor binding in forebrain regions: Correlations with social interest in brain region- and sex- specific ways. Horm Behav. https://doi.org/10.1016/j.yhbeh.2013.08.012
Duque-Wilckens N, Steinman MQ, Busnelli M, Chini B, Yokoyama S, Pham M, Laredo SA, Hao R, Perkeybile AM, Minie VA, Tan PB, Bales KL, Trainor BC (2018) Oxytocin receptors in the anteromedial bed nucleus of the stria terminalis promote stress-induced social avoidance in female California mice. Biol Psychiatry 83(3):203–213. https://doi.org/10.1016/j.biopsych.2017.08.024
Duque-Wilckens N, Torres LY, Yokoyama S, Minie VA, Tran AM, Petkova SP, Hao R, Ramos-Maciel S, Rios RA, Jackson K, Flores-Ramirez FJ, Garcia-Carachure I, Pesavento PA, Iniguez SD, Grinevich V, Trainor BC (2020) Extrahypothalamic oxytocin neurons drive stress-induced social vigilance and avoidance. Proc Natl Acad Sci U S A 117(42):26406–26413. https://doi.org/10.1073/pnas.2011890117
Freeman AR, Hare JF, Caldwell HK (2019) Central distribution of oxytocin and vasopressin 1a receptors in juvenile Richardson's ground squirrels. J Neurosci Res 97(7):772–789. https://doi.org/10.1002/jnr.24400
Freeman AR, Aulino EA, Caldwell HK, Ophir AG (2020) Comparison of the distribution of oxytocin and vasopressin 1a receptors in rodents reveals conserved and derived patterns of nonapeptide evolution. J Neuroendocrinol 32(4):e12828. https://doi.org/10.1111/jne.12828
Fricker BA, Seifert AW, Kelly AM (2021) Characterization of social behavior in the spiny mouse, *Acomys cahirinus*. Ethology 00:1–15
Froemke RC, Young LJ (2021) Oxytocin, neural plasticity, and social behavior. Annu Rev Neurosci 44:359–381. https://doi.org/10.1146/annurev-neuro-102320-102847
Frynta D, Frankova M, Cizkova B (2011) Social and life history correlates of litter size in captive colonies of precocial spiny mice (*Acomys*). Acta Theriol 56:289–295
Gawriluk TR, Simkin J, Thompson KL, Biswas SK, Clare-Salzler Z, Kimani JM, Kiama SG, Smith JJ, Ezenwa VO, Seifert AW (2016) Comparative analysis of ear-hole closure identifies epimorphic regeneration as a discrete trait in mammals. Nat Commun 7:11164. https://doi.org/10.1038/ncomms11164
Gonet AE, Stauffacher W, Pictet R, Renold AE (1966) Obesity and diabetes mellitus with striking congenital hyperplasia of the islets of Langerhans in spiny mice (Acomys Cahirinus): I. Histological findings and preliminary metabolic observations. Diabetologia 1(3–4):162–171. https://doi.org/10.1007/BF01257907
Gonzalez Abreu JA, Rosenberg AE, Fricker BA, Wallace KJ, Seifert AW, Kelly AM (2022) Species-typical group size differentially influences social reward neural circuitry during nonreproductive social interactions. iScience. https://doi.org/10.1016/j.isci.2022.104230
Goodson JL, Schrock SE, Klatt JD, Kabelik D, Kingsbury MA (2009) Mesotocin and nonapeptide receptors promote estrildid flocking behavior. Science 325(5942):862–866. https://doi.org/10.1126/science.1174929
Goodson JL, Thompson RR (2010) Nonapeptide mechanisms of social cognition, behavior and species-specific social systems. Curr Opin Neurobiol 20(6):784–794. https://doi.org/10.1016/j.conb.2010.08.020
Harmon AC, Huhman KL, Moore TO, Albers HE (2002) Oxytocin inhibits aggression in female Syrian hamsters. J Neuroendocrinol 14(12):963–969. https://doi.org/10.1046/j.1365-2826.2002.00863.x
Hashikawa K, Hashikawa Y, Tremblay R, Zhang J, Feng JE, Sabol A, Piper WT, Lee H, Rudy B, Lin D (2017) Esr1(+) cells in the ventromedial hypothalamus control female aggression. Nat Neurosci 20(11):1580–1590. https://doi.org/10.1038/nn.4644
Haughton CL, Gawriluk TR, Seifert AW (2016) The biology and husbandry of the African Spiny Mouse (*Acomys cahirinus*) and the research uses of a laboratory colony. J Am Assoc Lab Anim Sci 55(1):9–17
Hong W, Kim DW, Anderson DJ (2014) Antagonistic control of social versus repetitive self-grooming behaviors by separable amygdala neuronal subsets. Cell 158(6):1348–1361. https://doi.org/10.1016/j.cell.2014.07.049
Inoue K, Ford CL, Horie K, Young LJ (2022) Oxytocin receptors are widely distributed in the prairie vole (Microtus ochrogaster) brain: Relation to social behavior, genetic polymorphisms, and the dopamine system. J Comp Neurol. https://doi.org/10.1002/cne.25382
Insel TR, Gelhard R, Shapiro LE (1991) The comparative distribution of forebrain receptors for neurohypophyseal peptides in monogamous and polygamous mice. Neuroscience 43(2–3):623–630
Insel TR, Wang ZX, Ferris CF (1994) Patterns of brain vasopressin receptor distribution associated with social organization in microtine rodents. J Neurosci 14(9):5381–5392
Ito R, Hayen A (2011) Opposing roles of nucleus accumbens core and shell dopamine in the modulation of limbic information processing. J Neurosci 31(16):6001–6007. https://doi.org/10.1523/JNEUROSCI.6588-10.2011
Kalamatianos T, Faulkes CG, Oosthuizen MK, Poorun R, Bennett NC, Coen CW (2010) Telencephalic binding sites for oxytocin

and social organization: a comparative study of eusocial naked mole-rats and solitary cape mole-rats. J Comp Neurol 518(10):1792–1813. https://doi.org/10.1002/cne.22302

Keebaugh AC, Barrett CE, Laprairie JL, Jenkins JJ, Young LJ (2015) RNAi knockdown of oxytocin receptor in the nucleus accumbens inhibits social attachment and parental care in monogamous female prairie voles. Soc Neurosci 10(5):561–570. https://doi.org/10.1080/17470919.2015.1040893

Kelly AM, Goodson JL (2014) Social functions of individual vasopressin-oxytocin cell groups in vertebrates: What do we really know? Front Neuroendocrinol 35(4):512–529. https://doi.org/10.1016/j.yfrne.2014.04.005

Kelly AM, Seifert AW (2021) Distribution of vasopressin and oxytocin neurons in the basal forebrain and midbrain of spiny mice (*Acomys cahirinus*). Neuroscience 468:16–28

Kenkel WM, Perkeybile AM, Carter CS (2017) The neurobiological causes and effects of alloparenting. Dev Neurobiol 77(2):214–232. https://doi.org/10.1002/dneu.22465

Koopmans T, van Beijnum H, Roovers EF, Tomasso A, Malhotra D, Boeter J, Psathaki OE, Versteeg D, van Rooij E, Bartscherer K (2021) Ischemic tolerance and cardiac repair in the spiny mouse (Acomys). NPJ Regen Med 6(1):78. https://doi.org/10.1038/s41536-021-00188-2

Leung CH, Goode CT, Young LJ, Maney DL (2009) Neural distribution of nonapeptide binding sites in two species of songbird. J Comp Neurol 513(2):197–208. https://doi.org/10.1002/cne.21947

Li Y, Mathis A, Grewe BF, Osterhout JA, Ahanonu B, Schnitzer MJ, Murthy VN, Dulac C (2017) Neuronal representation of social information in the medial amygdala of awake behaving mice. Cell 171 (5):1176–1190 e1117. https://doi.org/10.1016/j.cell.2017.10.015

Lim MM, Wang Z, Olazabal DE, Ren X, Terwilliger EF, Young LJ (2004) Enhanced partner preference in a promiscuous species by manipulating the expression of a single gene. Nature 429(6993):754–757. https://doi.org/10.1038/nature02539

Lin D, Boyle MP, Dollar P, Lee H, Lein ES, Perona P, Anderson DJ (2011) Functional identification of an aggression locus in the mouse hypothalamus. Nature 470(7333):221–226. https://doi.org/10.1038/nature09736

Liu Y, Curtis JT, Wang Z (2001) Vasopressin in the lateral septum regulates pair bond formation in male prairie voles (*Microtus ochrogaster*). Behav Neurosci 115(4):910–919

Liu Y, Wang ZX (2003) Nucleus accumbens oxytocin and dopamine interact to regulate pair bond formation in female prairie voles. Neuroscience 121(3):537–544

Ludwig M, Leng G (2006) Dendritic peptide release and peptide-dependent behaviours. Nat Rev Neurosci 7(2):126–136. https://doi.org/10.1038/nrn1845

Mitre M, Marlin BJ, Schiavo JK, Morina E, Norden SE, Hackett TA, Aoki CJ, Chao MV, Froemke RC (2016) A Distributed network for social cognition enriched for oxytocin receptors. J Neurosci 36(8):2517–2535. https://doi.org/10.1523/JNEUROSCI.2409-15.2016

Newman SW (1999) The medial extended amygdala in male reproductive behavior. A node in the mammalian social behavior network. Ann N Y Acad Sci 877:242–257

Nogueira-Rodrigues J, Leite SC, Pinto-Costa R, Sousa SC, Luz LL, Sintra MA, Oliveira R, Monteiro AC, Pinheiro GG, Vitorino M, Silva JA, Simao S, Fernandes VE, Provaznik J, Benes V, Cruz CD, Safronov BV, Magalhaes A, Reis CA, Vieira J, Vieira CP, Tiscornia G, Araujo IM, Sousa MM (2022) Rewired glycosylation activity promotes scarless regeneration and functional recovery in spiny mice after complete spinal cord transection. Dev Cell 57 (4):440–450 e447. https://doi.org/10.1016/j.devcel.2021.12.008

Nowak RM (1999) Walker's mammals of the world. John Hopkins University Press, Baltimore

O'Connell LA, Hofmann HA (2011) The vertebrate mesolimbic reward system and social behavior network: a comparative synthesis. J Comp Neurol 519(18):3599–3639. https://doi.org/10.1002/cne.22735

O'Connell LA, Hofmann HA (2012) Evolution of a vertebrate social decision-making network. Science 336(6085):1154–1157. https://doi.org/10.1126/science.1218889

Okamura DM, Brewer CM, Wakenight P, Bahrami N, Bernardi K, Tran A, Olson J, Shi X, Yeh SY, Piliponsky A, Collins SJ, Nguyen ED, Timms AE, MacDonald JW, Bammler TK, Nelson BR, Millen KJ, Beier DR, Majesky MW (2021) Spiny mice activate unique transcriptional programs after severe kidney injury regenerating organ function without fibrosis. iScience 24(11):103269. https://doi.org/10.1016/j.isci.2021.103269

Olazabal DE, Sandberg NY (2020) Variation in the density of oxytocin receptors in the brain as mechanism of adaptation to specific social and reproductive strategies. Gen Comp Endocrinol 286:113337. https://doi.org/10.1016/j.ygcen.2019.113337

Paxinos G, Franklin KBJ (2012) The mouse brain in stereotaxic coordinates. 4ed. Elsevier

Peng H, Shindo K, Donahue RR, Gao E, Ahern BM, Levitan BM, Tripathi H, Powell D, Noor A, Elmore GA, Satin J, Seifert AW, Abdel-Latif A (2021) Adult spiny mice (Acomys) exhibit endogenous cardiac recovery in response to myocardial infarction. NPJ Regen Med 6(1):74. https://doi.org/10.1038/s41536-021-00186-4

Porter RH, Cavallaro SA, Moore JD (1980) Developmental parameters of mother-offspring interactions in *Acomys cahirinus*. Z Tierpsychol 53(2):153–170

Powell JM, Plummer NW, Scappini EL, Tucker CJ, Jensen P (2019) DEFiNE: a method for enhancement and quantification of fluorescently labeled axons. Front Neuroanat 12:117. https://doi.org/10.3389/fnana.2018.00117

Prounis GS, Thomas K, Ophir AG (2018) Developmental trajectories and influences of environmental complexity on oxytocin receptor and vasopressin 1A receptor expression in male and female prairie voles. J Comp Neurol 526(11):1820–1842. https://doi.org/10.1002/cne.24450

Rigney N, de Vries GJ, Petrulis A, Young LJ (2022) Oxytocin, vasopressin, and social behavior: from neural circuits to clinical opportunities. Endocrinology. https://doi.org/10.1210/endocr/bqac111

Rood BD, De Vries GJ (2011) Vasopressin innervation of the mouse (*Mus musculus*) brain and spinal cord. J Comp Neurol 519(12):2434–2474. https://doi.org/10.1002/cne.22635

Ross HE, Freeman SM, Spiegel LL, Ren X, Terwilliger EF, Young LJ (2009) Variation in oxytocin receptor density in the nucleus accumbens has differential effects on affiliative behaviors in monogamous and polygamous voles. J Neurosci 29(5):1312–1318. https://doi.org/10.1523/JNEUROSCI.5039-08.2009

Rossi LM, Reverte I, Ragozzino D, Badiani A, Venniro M, Caprioli D (2020) Role of nucleus accumbens core but not shell in incubation of methamphetamine craving after voluntary abstinence. Neuropsychopharmacology 45(2):256–265. https://doi.org/10.1038/s41386-019-0479-4

Saxena S, Vekaria H, Sullivan PG, Seifert AW (2019) Connective tissue fibroblasts from highly regenerative mammals are refractory to ROS-induced cellular senescence. Nat Commun 10(1):4400. https://doi.org/10.1038/s41467-019-12398-w

Schindelin J, Arganda-Carreras I, Frise E, Kaynig V, Longair M, Pietzsch T, Preibisch S, Rueden C, Saalfeld S, Schmid B, Tinevez JY, White DJ, Hartenstein V, Eliceiri K, Tomancak P, Cardona A (2012) Fiji: an open-source platform for biological-image analysis. Nat Methods 9(7):676–682. https://doi.org/10.1038/nmeth.2019

Seifert AW, Kiama SG, Seifert MG, Goheen JR, Palmer TM, Maden M (2012) Skin shedding and tissue regeneration in African spiny

mice (*Acomys*). Nature 489(7417):561–565. https://doi.org/10.1038/nature11499

Shafrir E (2000) Overnutrition in spiny mice (Acomys cahirinus): beta-cell expansion leading to rupture and overt diabetes on fat-rich diet and protective energy-wasting elevation in thyroid hormone on sucrose-rich diet. Diabetes Metab Res Rev 16(2):94–105. https://doi.org/10.1002/(sici)1520-7560(200003/04)16:2%3c94::aid-dmrr82%3e3.0.co;2-u

Sharma K, LeBlanc R, Haque M, Nishimori K, Reid MM, Teruyama R (2019) Sexually dimorphic oxytocin receptor-expressing neurons in the preoptic area of the mouse brain. PLoS ONE 14(7):e0219784. https://doi.org/10.1371/journal.pone.0219784

Sheng ZH, Cai Q (2012) Mitochondrial transport in neurons: impact on synaptic homeostasis and neurodegeneration. Nat Rev Neurosci 13(2):77–93. https://doi.org/10.1038/nrn3156

Smith CJ, Poehlmann ML, Li S, Ratnaseelan AM, Bredewold R, Veenema AH (2017) Age and sex differences in oxytocin and vasopressin V1a receptor binding densities in the rat brain: focus on the social decision-making network. Brain Struct Funct 222(2):981–1006. https://doi.org/10.1007/s00429-016-1260-7

Suzuki R, Terada Y, Shimodaira H (2019) pvclust: hierarchical clustering with p-values via multiscale bootstrap resampling. R package version 2.2–0. https://cran.r-project.org/web/packages/pvclust/pvclust.pdf

Taylor JH, McCann KE, Ross AP, Albers HE (2020) Binding affinities of oxytocin, vasopressin and Manning compound at oxytocin and V1a receptors in male Syrian hamster brains. J Neuroendocrinol 32(7):e12882. https://doi.org/10.1111/jne.12882

Team RC (2013) R: A language and environment for statistical computing. R Foundation for Statistical Computing, Vienna, Austria ISBN 3–900051–07–0

Tong WH, Abdulai-Saiku S, Vyas A (2020) Medial amygdala arginine vasopressin neurons regulate innate aversion to cat odors in male mice. Neuroendocrinology. https://doi.org/10.1159/000508862

Tribollet E, Barberis C, Dubois-Dauphin M, Dreifuss JJ (1992a) Localization and characterization of binding sites for vasopressin and oxytocin in the brain of the guinea pig. Brain Res 589(1):15–23. https://doi.org/10.1016/0006-8993(92)91156-9

Tribollet E, Dubois-Dauphin M, Dreifuss JJ, Barberis C, Jard S (1992b) Oxytocin receptors in the central nervous system. Distribution, development, and species differences. Ann N Y Acad Sci 652:29–38. https://doi.org/10.1111/j.1749-6632.1992.tb34343.x

Tuckova V, Sumbera R, Cizkova B (2016) Alloparental behaviour in Sinai spiny mice (*Acomys dimidiatus*): a case of misdirected parental care? Behav Ecol Sociobiol 70(3):437–447

Veenema AH, Neumann ID (2008) Central vasopressin and oxytocin release: regulation of complex social behaviours. Prog Brain Res 170:261–276. https://doi.org/10.1016/S0079-6123(08)00422-6

Walum H, Young LJ (2018) The neural mechanisms and circuitry of the pair bond. Nat Rev Neurosci 19(11):643–654. https://doi.org/10.1038/s41583-018-0072-6

Yoshimura R, Kiyama H, Kimura T, Araki T, Maeno H, Tanizawa O, Tohyama M (1993) Localization of oxytocin receptor messenger ribonucleic acid in the rat brain. Endocrinology 133(3):1239–1246. https://doi.org/10.1210/endo.133.3.8396014

Young LJ, Frank A (1999) Beach award. Oxytocin and vasopressin receptors and species-typical social behaviors. Horm Behav 36(3):212–221. https://doi.org/10.1006/hbeh.1999.1548

Young LJ, Wang Z (2004) The neurobiology of pair bonding. Nat Neurosci 7(10):1048–1054. https://doi.org/10.1038/nn1327

Zann RA (1996) The Zebra Finch: A Synthesis of Field and Laboratory Studies. Oxford University Press, USA